CMS Results on Diffraction

Albert Knutsson
DESY, Notkerstrasse 85, 22765 Hamburg

An overview of measurements of diffraction performed with the CMS detector at LHC is presented. The results include observations of diffraction in pp collisions at $\sqrt{s}$ =0.9, 2.36 and 7 TeV in minimum bias events, and in events with W and Z bosons at $\sqrt{s}$ = 7 TeV. The cross-section for diffractive di-jet production is presented as a function of $\tilde{\xi}$, a variable which approximates the fraction of the momentum loss of the proton. For completeness non-diffractive measurements of the energy flow at large rapidities are also shown.

1 Introduction

Hard diffraction was studied in detail at HERA in the end of the 20th century. By introducing a color singlet exchange, the Pomeron, and diffractive parton density functions the large rapidity gap events were successfully described at HERA. At LHC where the collision energies are higher, and particles with internal structure are collided, the picture complicates. One or several rapidity gaps may occur in the collisions from multiplicity fluctuations in the event or by exchange of color singlet objects. However, the survival probability of the rapidity gap may decrease due to multi-parton interactions (MPI), where additional remnant-remnant or proton-remnant interactions in the event produce radiation into the rapidity gap. Experimentally it may be hard to distinguish a non-diffractive event from a diffractive event where the rapidity gap is destroyed by MPI. Thus, a good understanding of MPI is crucial in order to understand the rapidity gap survival probability. The presented measurements are based on measuring the energy flow in the forward regions, and are performed at different center-of-mass energies and for events with different hard scales. In addition, the diffractive di-jet cross-section is presented. Because of the importance of understanding the contribution from MPI and the underlying event in the region of the detector were rapidity gaps are required, also non-diffractive measurements of energy flow in the forward region are included in these proceedings.

2 The CMS Detector

The CMS detector is described in detail in Ref. [1]. The most relevant detector component for the presented analyses is the Hadronic Forward calorimeters (HF), which cover the region of $2.9< |\eta| <5.2$. Each calorimeter is located 11.2 m from the interaction point, one on either side of CMS. The HF calorimeters consist of iron absorbers and embedded radiation-hard quartz fibres, providing a fast collection of Čherenkov light. The different length of the fibres makes it possible to distinguish electromagnetic showers from hadronic ones. The activity in the forward region are measured, by summing all energy deposits in the HF calorimeters.

The data were collected with the CMS detector during 2010 at different centre-of-mass energies. The corresponding integrated luminosities varies between 36 pb^{-1} and 240 μb^{-1} depending on center-of-mass energy and measurement. The detailed numbers are given within the references.

3 Results

3.1 Energy deposit in the HF calorimeter

In Refs. [2,3,4] the distributions of the total energy deposit in the HF calorimeter were measured. The measurements were performed for MB events collected at $\sqrt{s} = 0.9, 2.36$ [2] and 7 TeV [3], and at $\sqrt{s} = 7$ TeV for events with a hard scale set by a central W or Z [4].

In Fig. 1 the distributions of the energy deposit in the HF are shown for MB events at different centre-of-mass energies. The lines represent Monte Carlo predictions with and without diffraction included in the event generation. For events with an energy deposit of less than 4 GeV in one of the HFs, i.e. events with a rapidity gap of at least 2 units in rapidity, diffraction is needed in order to describe the data. In the same bin, the non-diffractive models predict too few events compared to data. The difference between the data and the non-diffractive predictions is a factor of 2-5 depending on the center-of-mass energy, and the diffractive component is somewhat larger for higher centre-of-mass energies.

The measurement was repeated at $\sqrt{s} = 7$ TeV for events with a central W or Z [4]. Here we focus on the W events which are the most statistically significant sample. Events with an isolated lepton of $p_t > 25$ GeV and $|\eta| < 1.4$, $E_{T,\text{miss}} > 30$ GeV and $m_{T(l,\nu)} > 60$ GeV were selected. Further details on selection and rejection criteria can be found in the reference. The final background to the selected events are less than 1%. The energy distribution in one of the HF calorimeters is shown in Fig. 2 for three different bins of energy deposits in the opposite HF calorimeter. When comparing the three distributions one notes a strong long range correlation, i.e. a larger energy deposit in the region $5.2 < -\eta < 3.2$ significantly increases the energy deposit in $3.2 < \eta < 5.2$. The data are compared to non-diffractive predictions from Pythia6 and Pythia8. The predictions from Pythia6 are made with different tunes and one can observe a large difference between the different tunes, in particular towards lower energies.

In opposite to the same measurement for MB events, diffraction is not needed in order to predict the number of events with $E < 4$ GeV in the forward region. However, when looking at the signed lepton pseudo rapidity distribution, η_l, for the same events, the shape of η_l can not be described by the non-diffractive Monte Carlo, and it is clear that diffraction is still present in the events with $E < 4$ GeV. This is shown in Fig. 3. A strong asymmetry is seen in the data. A possible explanation is that the diffractive PDF peaks at smaller momentum fractions of the proton, x, than the conventional PDF, and the W is thus boosted in the direction opposite to the rapidity gap. The measurement is compared to non-diffractive Monte Carlo predictions and a mixture of non-diffractive and diffractive Monte Carlo predictions. The mixture of the diffractive and non-diffractive contributions are determined by fitting the fraction to the data. The diffractive component is determined to be $(50.0 \pm 9.3(stat) \pm 5.2(syst))\%$ of the events in the bin with $E < 4$ GeV.

The fact that diffractive MC is not needed to describe the energy distribution can mean that either the requirement of $E < 4$ GeV in the rapidity gap is not exclusive enough, or the rapidity gaps are destroyed by MPI. In the latter case it is possible that the diffractive kinematics in the events are still observed.

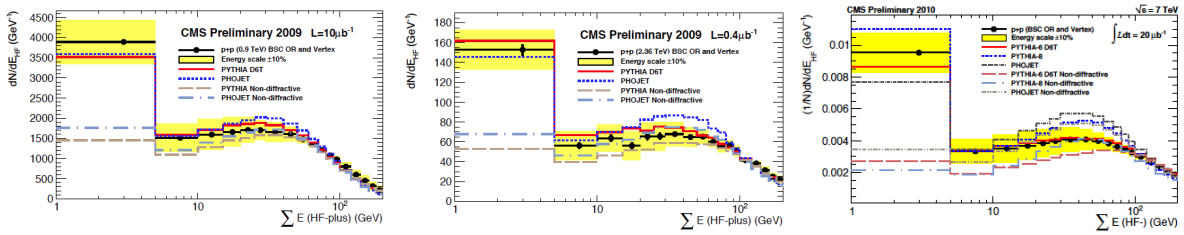

Figure 1: Distribution of minimum bias events as a function of the energy deposit in the Hadronic Forward calorimeters for $\sqrt{s}$ =0.9 (left), 2.36 (middle) and 7 TeV (right). The data are compared to non-diffractive and diffractive Monte Carlo predictions from PYTHIA6 and PHOJET.

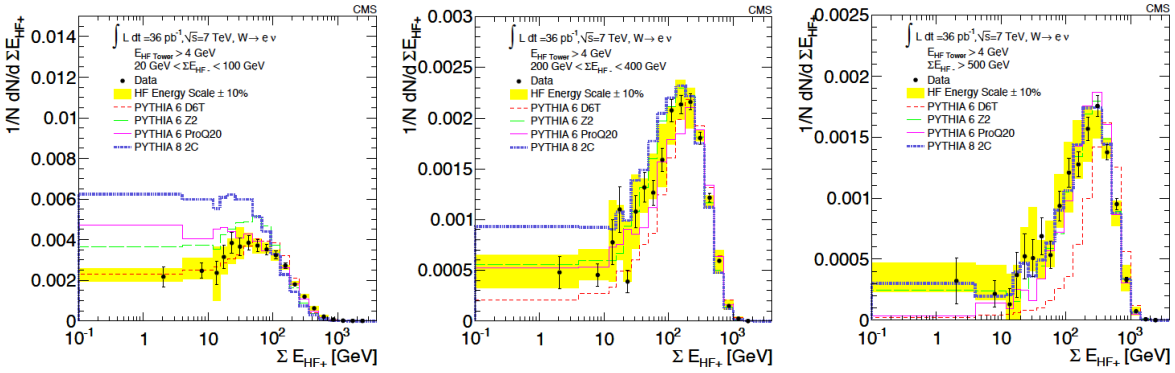

Figure 2: Distribution of events with a W as a function of the energy deposit in the Hadronic Forward calorimeters in three different bins of the energy deposit in the Hadronic Forward calorimeter on the opposite side in rapidity. The data are compared to non-diffractive Monte Carlo predictions from PYTHIA6 and PYTHIA8.

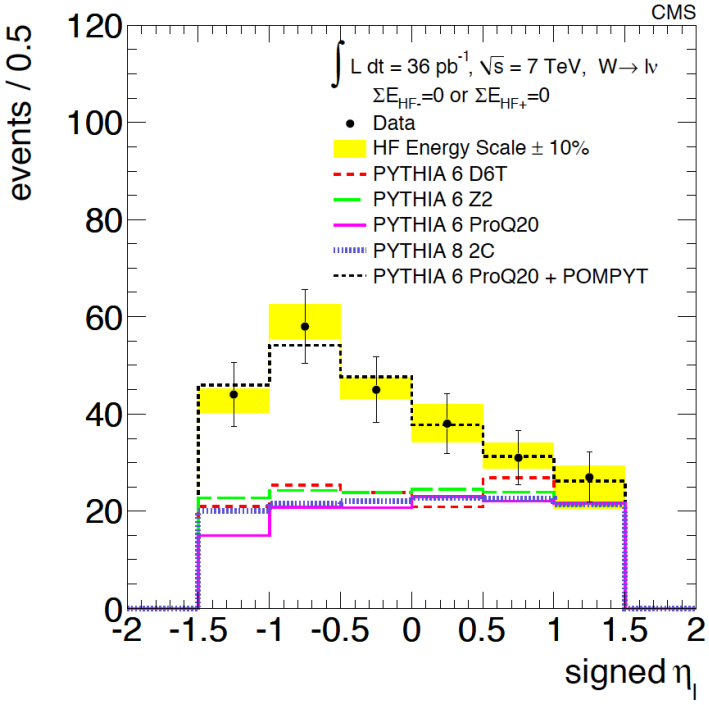

Figure 3: Signed lepton pseudo rapidity distribution, η_l, in W events with a large rapidity gap. The sign of η_l is positive (negative) if the lepton is in the same (opposite) hemisphere as the gap. The data are compared to non-diffractive predictions from PYTHIA6 (different tunes) and a diffractive prediction from PYTHIA6+POMPYT. The normalization of the PYTHIA6 predictions are determined by fitting the fraction of the non-diffraction component.

3.2 Non-diffractive energy flow in the HF calorimeter

In the measurement of energy flow as a function pseudo rapidity [5], the diffractive component in the data is suppressed by selecting events with at least one particle in coincidence in both of the BSC detectors. The data is fully corrected for detector effects to a particle level where a similar selection has been applied (see [5] for details). The selection suppresses rapidity gap events, and thus the analysis is a good study of how well non-diffraction is understood in the forward region. The analysis is performed at $\sqrt{s} = 0.9$ and 7 TeV, for MB events and for events with a central di-jet system ($|\eta| < 2.5$, $p_{t,jet} > 25$ GeV) . The results are shown in Fig. 4. The yellow band in the figure represents the spread of six different PYTHIA6 tunes (decomposed in [5]), while the lines represent other generators as indicated in the legends. Just as for the three earlier presented measurements of the energy deposit in the forward region there is a large model and tune dependence in the description of the data. Also observed is that there is a large contribution from MPI, which is 50-60%. Interesting is that several different cosmic ray Monte Carlo generators describe the measurement well at both center-of-mass energies and for both types of events (not shown).

3.3 Diffractive di-jet production

The cross-section for diffractive events with a di-jet system is presented in [6]. In the measurement, events with at least two jets with transverse momentum $p_{t,jet} > 20$ GeV and $|\eta| < 4.4$ were selected, and the cross-section was measured differentially in bins of $\tilde{\xi}$, defined as $\tilde{\xi}^{\pm} = \sum(E^i \pm p_z^i)/s$, where E^i and p_z^i are the energy and transverse momentum of the i^{th} particle in the system X. The "+" and "−" conventions account for the asymmetry in the reaction and are used for particles with $\eta^i < 4.9$ and $\eta^i > -4.9$, respectively. At low values $\tilde{\xi}$ approximates $\xi = M_X^2/s$.

Fig. 5 (right) shows the cross-section as a function of $\tilde{\xi}$. The data are compared to non-diffractive (PYTHIA6 Z2 and PYTHIA8 tune 1) and diffractive (POMPYT SD, POMWIG SD, PYTHIA8 SD+DD) Monte Carlo predictions. The non-diffractive Monte Carlo predictions underestimate the data at low $\tilde{\xi}$, but describes the data at higher $\tilde{\xi}$, i.e. higher $\tilde{\xi}$ is dominated by non-diffractive events. On the other hand, the diffractive predictions from PYTHIA8 with POMPYT or POMWIG overestimates the data significantly at all $\tilde{\xi}$, while the prediction from PYTHIA8 SD+DD underestimates the data. The difference between the generators are that POMPYT and POWHEG use diffractive parton distributions and a parameterization of the Pomeron flux from fits to HERA data, which is not the case for PYTHIA8. The overestimate of the diffractive cross-section in POMPYT and POWHEG can be used to estimate the gap survival probability, which are not simulated by the generators. Assuming a contribution of 41% proton dissociation in the data, gives a survival probability of 0.12 ± 0.05.

4 Summary

The presented measurements span a large range of energies, final states and different hardness of reactions. The measurements of the energy deposit in the forward region show a large difference between MB and W/Z events. Hard diffraction is needed in order to predict the number of rapidity gap events in MB events, while the non-diffractive Monte Carlo is in agreement with the W/Z data. However, when looking at the signed lepton distribution in W events with large rapidity gaps, the asymmetry in the data can only be described when the appropriate mix of diffractive and non-diffractive Monte Carlo is used (about 50%). Thus, hard diffraction is present in the W events, but diffraction is not needed to predict the number of events with large rapidity gaps.

Furthermore, the di-jet production in events with hard diffraction is measured. The overestimate of the diffractive cross-sections, by diffractive Monte Carlo, shows that the factorization

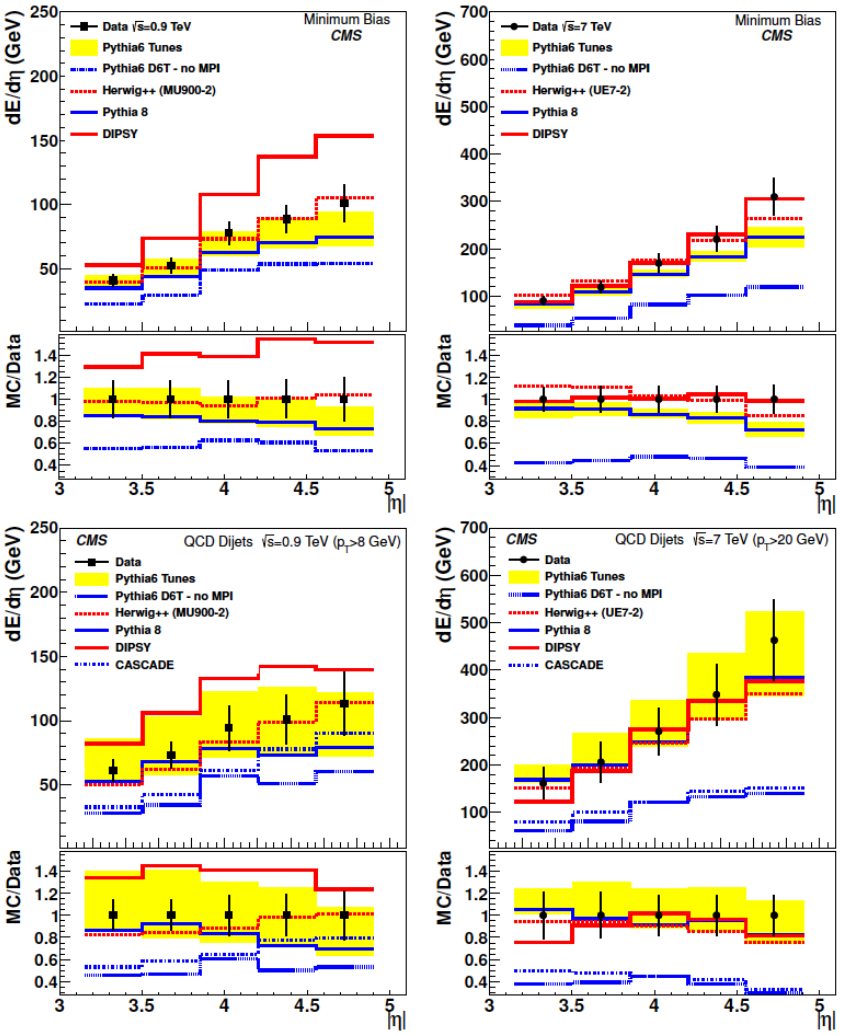

Figure 4: Energy flow as a function of for minimum-bias (upper) and dijet (lower) events at s = 0.9TeV and s = 7 TeV. The data are shown as points with error bars, while the histograms correspond to predictions obtained from different Monte Carlo event generators. The error bars represent the systematic uncertainties, which are strongly correlated between the bins. The statistical uncertainties are negligible. The lower panels show the ratio of Monte Carlo prediction to data.

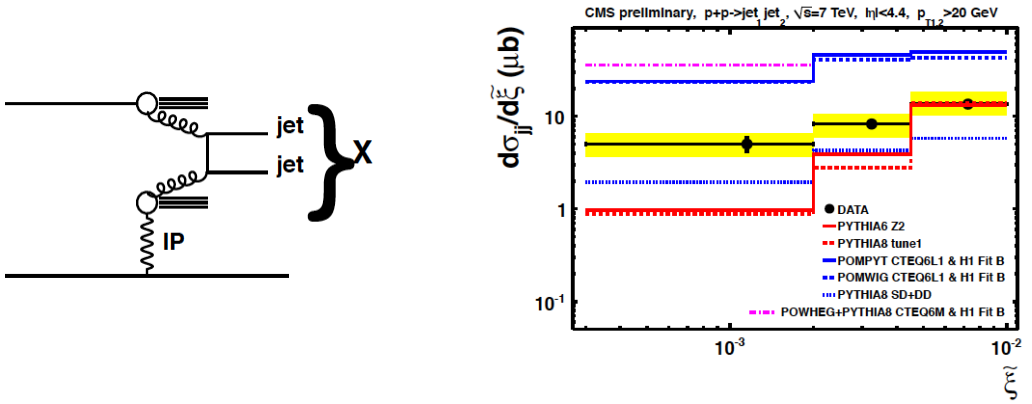

Figure 5: The left figure illustrates diffractive di-jet production. The right figure shows the differential dijet cross-section as a function of $\tilde{\xi}$ for events with a dijet system with $|\eta| < 4.4$ and $p_T > 20$ GeV for respectively jet. The error bars indicate the statistical uncertainty and the band represents the systematic uncertainties added in quadrature. The data are compared to predictions from non-diffractive (PYTHIA6 Z2 and PYTHIA8 tune 1) and diffractive (POMPYT SD, POMWIG SD and PYTHIA8 SD+DD) Monte Carlo. The first bin shows also a NLO calculation based on POWHEG.

breaking is not properly modulated, which can be due to the fact that MPI is not yet modeled in diffractive events in the MC. Also, from the non-diffractive measurements of energy flow as a function of pseudo rapidity we learn that the contribution from MPI is very important in the region where we measure the rapidity gaps.

1. S. Chatrchyan *et al.* [CMS Collaboration], JINST **3** (2008) S08004.
2. CMS PAS FWD-10-001, http://cdsweb.cern.ch/record/1328610
3. CMS PAS FWD-10-007, http://cdsweb.cern.ch/record/1328610
4. S. Chatrchyan *et al.* [CMS Collaboration], Eur. Phys. J. C **72** (2012) 1839 [arXiv:1110.0181 [hep-ex]].
5. S. Chatrchyan *et al.* [CMS Collaboration], JHEP **1111** (2011) 148 [Erratum-ibid. **1202** (2012) 055] [arXiv:1110.0211 [hep-ex]].
6. CMS PAS FWD-10-004, http://cdsweb.cern.ch/record/1421606